JOURNAL OF COMPUTATIONAL PHYSICS 104, 321–328 (1993)

Simultaneous Potential and Circuit Solution for 1D Bounded Plasma Particle Simulation Codes

J. P. VERBONCOEUR

University of California, Berkeley, California 94720

M. V. ALVES

Institute for Space Research (INPE), S. J. dos Campos, SP, 12201, Brazil

AND

V. VAHEDI AND C. K. BIRDSALL

University of California, Berkeley, California 94720

Received September 19, 1990; revised December 26, 1991

A general second-order accurate method for solving the combined potential and circuit equations in a one-dimensional electrostatic bounded plasma PIC simulation is presented. The boundary conditions include surface charge on the electrodes, which are connected to a series RLC circuit with driving terms $V(t)$ or $I(t)$. The solution is obtained for planar, cylindrical, and spherical electrodes. The result is a tridiagonal matrix which is readily solved using well-known methods. The method is implemented in the codes PDP1 (plasma device planar 1D), PDC1 (cylindrical), and PDS1 (spherical).

1. INTRODUCTION

A comprehensive review of the considerations involved in bounded plasma particle simulation is presented by W. S. Lawson [1]. Lawson presents a method for solving the circuit equation which is second-order accurate when $\Delta t^2/LC \ll 1$ and $R\,\Delta t/L \ll 1$ and is stable for $\Delta t^2/LC < 2$ and $R\,\Delta t/L < 2$. Lawson's method is first-order accurate, with some modifications to improve the accuracy, when $L \to 0$ and the external circuit solution is no longer known at the same time as the charge density of the plasma. In addition, Lawson proposes a second-order accurate method for an RC external circuit. We describe a similar method which we extend to handle all variations of voltage and current driven series RLC circuits as well as solving the circuit equations simultaneously (in phase) with the plasma Poisson equation.

In [1, 2] the boundary conditions are decoupled from the potential equation and a first-order circuit solution is used when the inductance is zero. The scheme is self-consistent when L is non-zero and the applied (driving) potential is small compared to the space-charge potential across the system. These conditions are violated for a large class of problems, including capacitively coupled RF discharges and plasma immersion ion implantation materials processing ($L = R = 0$ and $C \to \infty$); therefore, an extension of Lawson's method is desired.

2. POTENTIAL EQUATION

The configuration for one-dimensional bounded plasma systems is shown in Fig. 1. The current in the external circuit interacts with the plasma current via surface charge on the electrodes. Similarly, the potential within the plasma region is affected by the distribution and motion of space charge, the electrode surface charge, and the current in the external circuit. Thus, we seek a simultaneous solution for the potential and circuit equations.

The boundary conditions for the potential equation are obtained by applying Gauss' law to the system [1],

$$\oint_S \mathbf{E} \cdot d\mathbf{S} = \int_V \frac{\rho}{\varepsilon}\, dV + \frac{A_+\sigma_+ + A_-\sigma_-}{\varepsilon} = 0, \qquad (1)$$

where the surface S encloses the plasma and electrodes. A_+ refers to the surface area of the left electrode, A_- to the right electrode, and σ is the surface charge on the respective electrode. Note that ρ has units of charge/volume and σ has units of charge/area. Equation (1) is a statement of Gauss' law; the first part reflects the assumption of an ideal conductor connecting the electrodes to the external circuit elements and the second part expresses conservation of charge in the system.

0021-9991/93 $5.00

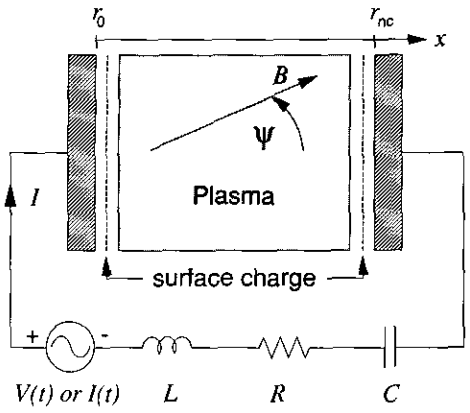

FIG. 1. One-dimensional configuration with series RLC circuit and voltage/current source. In these coordinates, the particles are charge sheets with motion in the r-direction. For planar coordinates, $r \to x$.

Applying Gauss' law about each node of the gridded system and using the definition of potential, we obtain planar

$$\frac{\Phi_{j+1}-2\Phi_j+\Phi_{j-1}}{\Delta x^2}=-\frac{\rho_j}{\varepsilon}, \tag{2a}$$

cylindrical

$$r_{j+1/2}\Phi_{j+1}-2r_j\Phi_j+r_{j-1/2}\Phi_{j-1}=-\frac{r_j\Delta r^2}{\varepsilon}\rho_j, \tag{2b}$$

and spherical

$$r_{j+1/2}^2\Phi_{j+1}-(r_{j+1/2}^2+r_{j-1/2}^2)\,\Phi_j+r_{j-1/2}^2\Phi_{j-1} =-\frac{(r_{j+1/2}^3-r_{j-1/2}^3)\,\Delta r}{3\varepsilon}\rho_j. \tag{2c}$$

In the cylindrical and spherical forms, $r_{j\pm1/2}=r_j\pm\Delta r/2$. For all Eqs. (2), $j=1, 2, ..., nc-1$, where nc is the number of cells in the gridded space. These results are equivalent to the flux-conserving method of Birdsall and Langdon [2]. The planar and cylindrical results of Eq. (2) can also be obtained by applying a central difference to the Poisson equation; the finite difference result is different in spherical coordinates.

For a one-dimensional system, the boundary conditions can be written

$$\Phi_{nc}=0 \tag{3}$$

and

$$E_0=\sigma_+/\varepsilon. \tag{4}$$

Equation (3) fixes a reference potential for the system without implying a grounded electrode. For the cylindrical and spherical models the inner electrode is driven. The outer electrode serves as the reference potential for the system even when the inner electrode is not present. Equation (4) can be written at one-half grid cell from the boundary, in conjunction with a central difference applied to the definition of potential, to obtain

planar

$$E_{1/2}=\frac{\Phi_0-\Phi_1}{\Delta x}=\frac{1}{\varepsilon}\left(\sigma_+ +\rho_0\frac{\Delta x}{2}\right), \tag{5a}$$

cylindrical

$$E_{1/2}=\frac{\Phi_0-\Phi_1}{\Delta r}=\frac{1}{\varepsilon}\left(\sigma_+\frac{r_0}{r_{1/2}}+\frac{\rho_0}{2}\left(r_{1/2}-\frac{r_0^2}{r_{1/2}}\right)\right), \tag{5b}$$

and spherical

$$E_{1/2}=\frac{\Phi_0-\Phi_1}{\Delta r}=\frac{1}{\varepsilon}\left(\sigma_+\frac{r_0^2}{r_{1/2}^2}+\frac{\rho_0}{3}\left(r_{1/2}-\frac{r_0^3}{r_{1/2}^2}\right)\right). \tag{5c}$$

Equations (2) and the boundary conditions for the gridded system are written in a general matrix form,

$$\begin{bmatrix} b_0 & c_0 & 0 & \cdot & \cdot & \cdot & \\ a_1 & b_1 & c_1 & 0 & & & \\ 0 & a_2 & b_2 & c_2 & 0 & & \\ \cdot & & \cdot & \cdot & \cdot & & \\ \cdot & & & \cdot & \cdot & \cdot & \\ \cdot & & & & \cdot & \cdot & \cdot \\ & & & & a_{nc-2} & b_{nc-2} & c_{nc-2} \\ & & & & & a_{nc-1} & b_{nc-1} \end{bmatrix} \times \begin{bmatrix} \Phi_0 \\ \Phi_1 \\ \Phi_2 \\ \cdot \\ \cdot \\ \cdot \\ \Phi_{nc-2} \\ \Phi_{nc-1} \end{bmatrix}^t = f \begin{bmatrix} d_0 \\ d_1 \\ d_2 \\ \cdot \\ \cdot \\ \cdot \\ d_{nc-2} \\ d_{nc-1} \end{bmatrix}^t . \tag{6}$$

The superscript indicates the quantity is evaluated at time t. The matrix elements in planar coordinates are

$$\begin{aligned} a_j&=1, \quad && j=1, 2, ..., nc-1; \\ b_0&=-1, \quad b_j=-2, && j=1, 2, ..., nc-1; \\ c_j&=1, && j=0, 1, ..., nc-2; \end{aligned} \tag{7}$$

$$d_0=\frac{\sigma_+^t}{\Delta x}+\frac{\rho_0^t}{2}, \quad d_j=\rho_j^t, \quad j=1, 2, ..., nc-1;$$

$$f=-\Delta x^2/\varepsilon.$$

The matrix elements in cylindrical coordinates are

$$\begin{aligned} & a_j = r_{j-1/2}, \quad j = 1, 2, ..., nc-1; \\ b_0 = -r_{1/2}, \quad & b_j = -2r_j, \quad j = 1, 2, ..., nc-1; \\ & c_j = r_{j+1/2}, \quad j = 0, 1, ..., nc-2; \end{aligned} \tag{8}$$

$$d_0 = \sigma^t_+ \frac{r_0}{\Delta r} + \frac{\rho^t_0}{2\Delta r}(r^2_{1/2} - r^2_0),$$

$$d_j = r_j \rho^t_j, \quad j = 1, 2, ..., nc-1;$$

$$f = -\Delta r^2/\varepsilon.$$

The matrix elements in spherical coordinates are

$$\begin{aligned} & a_j = r^2_{j-1/2}, && j = 1, 2, ..., nc-1; \\ b_0 = -r^2_{1/2}, \quad & b_j = -(r^2_{j-1/2} + r^2_{j+1/2}), && j = 1, 2, ..., nc-1; \\ & c_j = r^2_{j+1/2}, && j = 0, 1, ..., nc-2; \end{aligned} \tag{9}$$

$$d_0 = 3\sigma^t_+ r^2_0 + \rho^t_0 (r^3_{1/2} - r^3_0),$$

$$d_j = (r^3_{j+1/2} - r^3_{j-1/2})\, \rho^t_j, \quad j = 1, 2, ..., nc-1;$$

$$f = -\Delta r/3\varepsilon.$$

When the center conductor is not present in the curvilinear models, the boundary conditions must be modified. There can be no return current, so the boundary conditions simplify to fixing a reference potential (e.g., $\Phi_{nc} = 0$) and $E_0 = 0$. The only modifications this imposes on our previous solution are the removal of the center electrode surface charge and fixing a reference potential. From Gauss' law, the electric field at the origin must be zero in one dimension. Integrating Gauss' law from the origin to $r = r_{1/2}$ with $\sigma_+ = 0$, we obtain the modified form of Eqs. (5) for the hollow cylindrical system [2, Section 14-10],

$$E_{1/2} = \frac{\Phi_0 - \Phi_1}{\Delta r} = \frac{1}{\varepsilon}\left(\frac{\rho_0}{2} r_{1/2}\right). \tag{10}$$

The coefficients are still given by Eqs. (8), with the modification that

$$d_0 = \frac{\rho^t_0}{2\Delta r} r^2_{1/2}. \tag{11}$$

The modification of Eqs. (9) for removal of the center electrode in the spherical system is, similarly,

$$d_0 = \rho^t_0 r^3_{1/2}. \tag{12}$$

3. CIRCUIT

The external circuit is coupled to Eqs. (6)–(9) through conservation of charge at each wall,

$$A\, \Delta\sigma = Q_{\text{conv}} + \Delta Q, \tag{13}$$

where Q_{conv} is the charge deposited by the convection (particle) current and ΔQ is the charge deposited by the external circuit current, both over some interval in time. Equation (13) is applied at the positively biased electrode as shown in Fig. 1, guaranteeing conservation of charge at all times. The same logic can also be applied to the other electrode; however, the surface charge on the second electrode is determined readily from Eq. (1) when the first surface charge is known. The charge conservation equation becomes

$$\sigma^t = \sigma^{t-\Delta t} + \frac{Q^t_{\text{conv}} + Q^t - Q^{t-\Delta t}}{A}, \tag{14}$$

where Q is the charge on one plate of the external circuit capacitor. An alternate method of coupling the circuit to the potential matrix is applying continuity of current (Kirchhoff's current law) at the boundary [2, Section 16–9],

$$\frac{\partial\sigma}{\partial t} = J_{\text{conv}} + \frac{I}{A}, \tag{15}$$

where J_{conv} is the plasma convection current at the electrode. The methods are equivalent when a first-order backward difference is used for $\partial\sigma/\partial t$ and $I = \partial Q/\partial t$. Since Q_{conv} is in general a noisy quantity in a particle simulation, any other quantity in Eqs. (13) and (15) will contain similar noise. Thus Eq. (13) causes the wall charge σ to be noisy as might be expected, because the capacitor charge reacts to the particle convection current only through the wall charge; i.e., particles absorbed by the wall contribute immediately to σ, but the charge drains slowly to the capacitor through currents. It can be shown that Eq. (15) results in the convection current being absorbed gradually into σ, so that the noise is induced in the capacitor charge Q (and consequently in the external current I) to satisfy conservation of charge. Therefore we use the conservation of charge method of Eq. (13).

3.1. *General Series RLC Circuit*

Four cases cover the full range of external circuit parameters. For the general voltage-driven series RLC circuit, the capacitor charge Q is advanced using Kirchoff's voltage law,

$$L\frac{d^2Q}{dt^2} + R\frac{dQ}{dt} + \frac{Q}{C} = V(t) + \Phi_{nc} - \Phi_0. \tag{16}$$

The polarity of the source and resultant positive current are shown in Fig. 1. The general circuit equation is finite differenced using the second-order backward Euler representation of the first derivative,

$$\left(\frac{dQ}{dt}\right)^t = \frac{3Q^t - 4Q^{t-\Delta t} + Q^{t-2\Delta t}}{2\Delta t}, \tag{17}$$

and the second derivative,

$$\left(\frac{d^2Q}{dt^2}\right)^t = \frac{3(dQ/dt)^t - 4(dQ/dt)^{t-\Delta t} + (dQ/dt)^{t-2\Delta t}}{2\Delta t} = \frac{9Q^t - 24Q^{t-\Delta t} + 22Q^{t-2\Delta t} - 8Q^{t-3\Delta t} + Q^{t-4\Delta t}}{4\Delta t^2}. \tag{18}$$

The latter is obtained by a second application of the first derivative to Q. An alternate four-point difference for the second derivative is given by

$$\left(\frac{d^2Q}{dt^2}\right)^t = \frac{2Q^t - 5Q^{t-\Delta t} + 4Q^{t-2\Delta t} - Q^{t-3\Delta t}}{\Delta t^2}. \tag{19}$$

The charge on the capacitor is not known at t. Combining Eqs. (16)–(18), we obtain

$$Q^t = \frac{V(t) + \Phi^t_{nc} - \Phi^t_0 - K^t}{\alpha_0}, \tag{20}$$

where

$$\begin{aligned} K^t &= \alpha_1 Q^{t-\Delta t} + \alpha_2 Q^{t-2\Delta t} + \alpha_3 Q^{t-3\Delta t} + \alpha_4 Q^{t-4\Delta t}, \\ \alpha_0 &= \frac{9}{4}\frac{L}{\Delta t^2} + \frac{3}{2}\frac{R}{\Delta t} + \frac{1}{C}, \\ \alpha_1 &= -6\frac{L}{\Delta t^2} - 2\frac{R}{\Delta t}, \\ \alpha_2 &= \frac{11}{2}\frac{L}{\Delta t^2} + \frac{1}{2}\frac{R}{2\Delta t}, \\ \alpha_3 &= -2\frac{L}{\Delta t^2}, \\ \alpha_4 &= \frac{1}{4}\frac{L}{\Delta t^2}. \end{aligned} \tag{21}$$

Combining the potential equation results, Eqs. (6)–(9), with the circuit equation results, Eqs. (20) and (21), using the boundary condition, Eq. (14), we obtain the self-consistent field solution matrix for the voltage-driven series RLC circuit case. The matrix can still be represented by Eq. (6), replacing elements of Eqs. (7)–(9) as follows: In the planar model,

$$\begin{aligned} b_0 &= -1 - \frac{\Delta x}{\alpha_0 \varepsilon A}, \\ d_0 &= \frac{\rho^t_0}{2} + \frac{\sigma^{t-\Delta t}_+}{\Delta x} + \frac{1}{A\,\Delta x}\left(Q^t_{\text{conv}} - Q^{t-\Delta t} + \frac{V(t) - K^t}{\alpha_0}\right). \end{aligned} \tag{22}$$

In the cylindrical model,

$$\begin{aligned} b_0 &= -r_{1/2} - \frac{\Delta r}{2\pi\varepsilon\alpha_0 h}, \\ d_0 &= \frac{r^2_{1/2} - r^2_0}{2\Delta r}\rho^t_0 + \frac{r_0}{\Delta r}\sigma^{t-\Delta t}_+ \\ &\quad + \frac{1}{2\pi h\,\Delta r}\left(Q^t_{\text{conv}} - Q^{t-\Delta t} + \frac{V(t) - K^t}{\alpha_0}\right). \end{aligned} \tag{23}$$

In the spherical model,

$$\begin{aligned} b_0 &= -r^2_{1/2} - \frac{\Delta r}{4\pi\varepsilon\alpha_0}, \\ d_0 &= (r^3_{1/2} - r^3_0)\rho^t_0 + 3r^2_0\sigma^{t-\Delta t}_+ \\ &\quad + \frac{3}{4\pi}\left(Q^t_{\text{conv}} - Q^{t-\Delta t} + \frac{V(t) - K^t}{\alpha_0}\right). \end{aligned} \tag{24}$$

Here, A is area of the planar electrodes and h is axial length of the cylindrical system. The solution is then self-consistent and second-order accurate for the general circuit case. The matrix can be solved using any algorithm optimized for tridiagonal matrices [3].

3.2. *Open Circuit (Floating Outer Electrode)*

When $C \to 0$, the impedance of the external circuit approaches infinity, becoming an open circuit. The potentials on the boundaries are floating; no circuit solution is required since there is no external current. The surface charges on the electrodes influence the potential as always, but the electrodes cannot exchange charge via external current. In this case, the field solution is given by Eqs. (6)–(9), with

$$\sigma^t_+ = \sigma^{t-\Delta t}_+ + Q^t_{\text{conv}}. \tag{25}$$

3.3. *Short-Circuit*

When $R = L = 0$ and $C \to \infty$, the external circuit is a short, with

$$\Phi_0 - \Phi_{nc} = V(t). \tag{26}$$

The short-circuit case is applied in practice when

planar

$$\frac{C}{\varepsilon A/l} > 10^5, \tag{27a}$$

cylindrical

$$\frac{C}{2\pi\varepsilon h/\ln(r_{nc}/r_0)} > 10^5, \tag{27b}$$

and spherical

$$\frac{C}{4\pi\varepsilon r_{nc} r_0/(r_{nc}-r_0)} > 10^5, \tag{27c}$$

where l is the length of the planar plasma region.

The field solution is still given by Eqs. (6)–(9), with

$$a_1 = b_0 = c_0 = d_0 = 0 \tag{28}$$

and

planar

$$d_1 = \rho_1^t - \frac{V(t)}{f}, \tag{29a}$$

cylindrical

$$d_1 = r_1 \rho_1^t - \frac{r_{1/2} V(t)}{f}, \tag{29b}$$

and spherical

$$d_1 = (r_{3/2}^3 - r_{1/2}^3)\, \rho_1^t - \frac{r_{1/2}^2 V(t)}{f}. \tag{29c}$$

Equation (28) eliminates the first row of Eq. (6). In Eq. (29), f depends on the model as given in Eqs. (7)–(9). Note that the wall charge is no longer required to solve the potential equation. Wall charge is found using Eq. (5), once the potentials have been determined, and the current is found by finite differencing Eq. (15),

$$I^{t-\Delta t/2} = A\left(J_{\text{conv}} + \frac{\sigma^t - \sigma^{t-\Delta t}}{\Delta t}\right). \tag{30}$$

Determining the current in this way produces a noisy result as discussed above; however, with a short between the electrodes, we expect large currents with rapid changes since potential differences cannot exist along an ideal conductor. Note that here I is only a diagnostic quantity, so the time-centering is not a problem.

3.4. *Current-Driven Circuit*

The final case is the current-driven external circuit. An ideal current source is assumed which can drive the specified time-varying current $I(t)$. The external circuit elements R, L, and C are ignored since an ideal current source is an open circuit. Then Eqs. (6)–(9) are applied with the wall charge found by finite differencing Eq. (15) for diagnostic purposes.

3.5. *Initial Conditions*

The multi-point finite difference methods require initial values for the Q^n, where $n \leqslant 0$. Physically, these values are used to obtain the desired initial conditions for the circuit equation, Eq. (16). For example, the initial charge on the capacitor, Q^0, and the initial current in the external circuit, I^0, form a complete set of initial conditions for the differential equation. However, the finite difference requires five initial values for Q (four for the four-point method). There are several ways the conditions can be obtained.

The traditional method for starting a multi-point scheme (second or higher order accurate) is to use a two-point method (first-order accurate) to obtain the required initial values. A smaller timestep is used with the two-point method to maintain the same accuracy. This presents a problem for a PIC code; the time-centered mover is initialized such that positions are known at integral timesteps, while velocities are known at half timesteps [2]. Thus, it is difficult to switch to a new Δt and maintain the time centering. Also, switching schemes is inefficient from a coding standpoint. In addition, the stability of the starter method must be considered in relation to the circuit parameters R, L, and C.

Another method of initializing the solver is to solve the circuit equations analytically. To do this, we must replace the plasma by a known impedance. Using the vacuum capacitance of the plasma region is the obvious choice; phisically, this means there is no plasma until $t = 0^+$. If plasma is then introduced, the impedance changes abruptly and the circuit has been conditioned for a different system. This problem is less severe when the plasma is generated at a slow rate since the impedance change is gradual.

If the method turns out to be stable, the initial conditions will be damped regardless of the value (this includes desired initial conditions as well as error in the initial conditions). If the method is unstable, any error in the initial conditions grows exponentially. If the method is marginally stable, any error in the initial conditions remains in the solution, neither growing nor damping.

3.6. *Stability*

We now explore stability of the circuit equation, Eq. (20). As is customary for stability analysis [4], we neglect the driving terms and study the homogeneous circuit equation

$$L\frac{d^2Q}{dt^2} + R\frac{dQ}{dt} + \frac{Q}{C} = 0. \tag{31}$$

We study the stability of the five-point circuit difference, Eqs. (17)–(18), as well as the four-point difference, Eqs. (17) and (19).

In the limit of no inductance, $L \to 0$, both methods produce

$$Q^t\left(3+\frac{2\Delta t}{RC}\right)-4Q^{t-\Delta t}+Q^{t-2\Delta t}=0. \tag{32}$$

Letting $Q^t = Q^0 e^{\gamma t}$ and $\xi = e^{\gamma \Delta t}$, we obtain

$$Q^t = \xi Q^{t-\Delta t} = \xi^2 Q^{t-2\Delta t}, \tag{33}$$

where $|\xi| \leqslant 1$ is required for stability. Here, γ and ξ are arbitrary complex variables. Then the characteristic stability equation for Eq. (32) is

$$\xi^2(3+2\Delta t/RC)-4\xi+1=0. \tag{34}$$

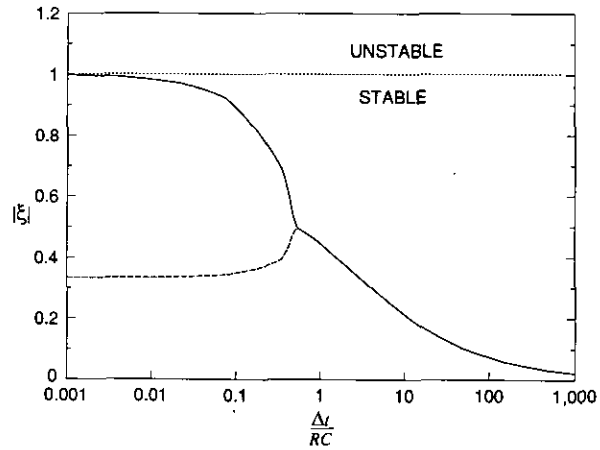

FIG. 2. Stability roots in the limit $L \to 0$. Since $|\xi| \leqslant 1$ everywhere, the method is stable. The scheme can only follow the RC time when $\Delta t \leqslant RC/2$.

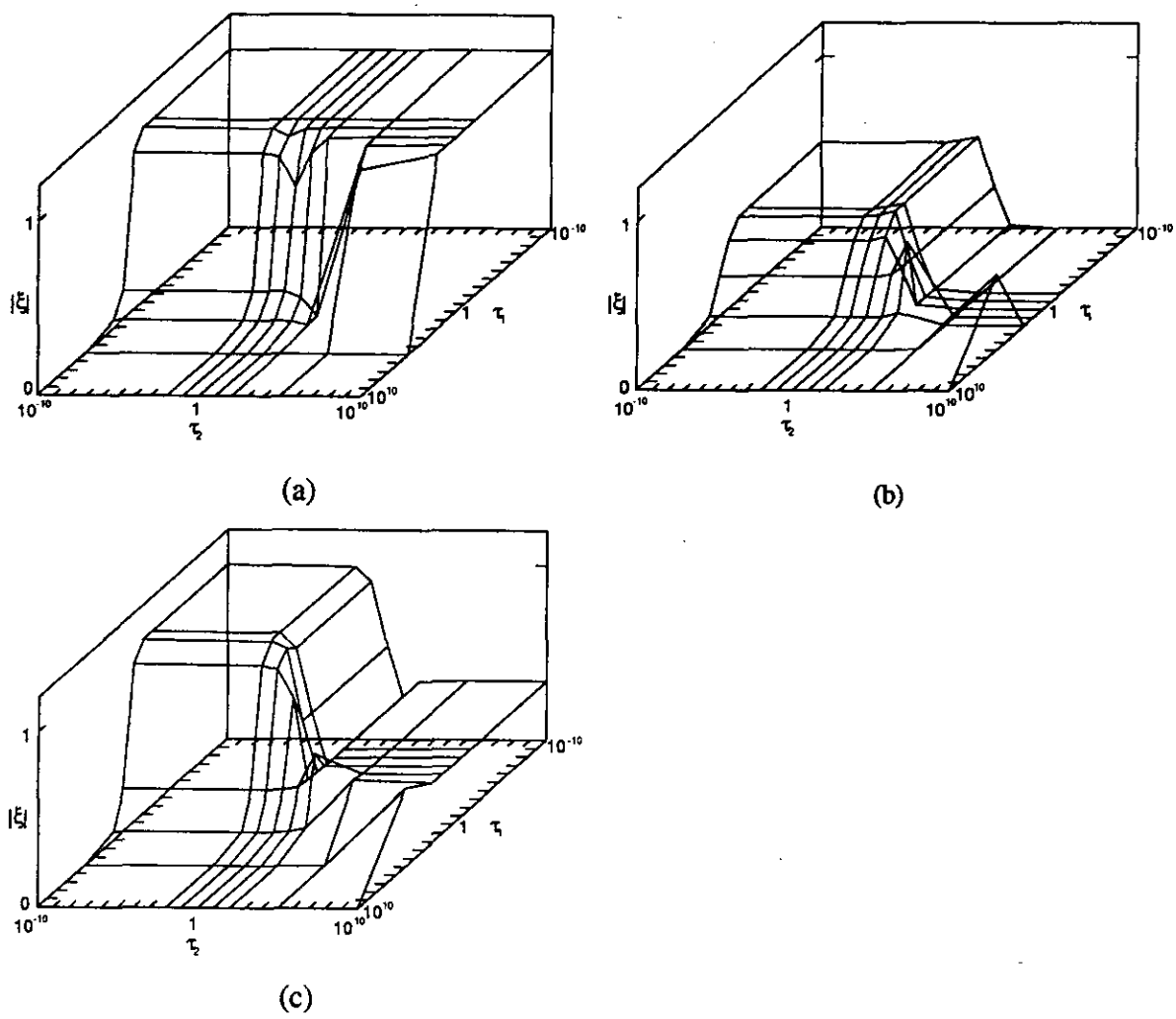

FIG. 3. Magnitude of the three roots of the four point method, whose characteristic equation is Eq. (36). Since for all three roots, $|\xi_{1,2,3}| \leqslant 1$, the four-point difference method is stable over the range shown.

The roots are

$$\xi = \frac{2 \pm \sqrt{1 - 2\Delta t/RC}}{3 + 2\Delta t/RC}. \tag{35}$$

As shown in Fig. 2, both methods are stable in the limit $L \to 0$ for all positive, real $\Delta t/RC$.

Now we attack the more difficult general case. The general characteristic stability equations for the four- and five-point schemes are respectively

$$\xi^3(2 + \tfrac{3}{2}\tau_1 + \tau_2^2) - \xi^2(5 + 2\tau_1) + \xi(4 + \tfrac{1}{2}\tau_1) - 1 = 0 \tag{36}$$

$$\xi^4(9 + 6\tau_1 + 4\tau_2^2) - \xi^3(24 + 8\tau_1) + \xi^2(22 + 2\tau_1) - 8\xi + 1 = 0, \tag{37}$$

where the normalized times are $\tau_1 = R\,\Delta t/L$ and $\tau_2 = \Delta t/\sqrt{LC}$. We obtain the roots of Eqs. (36) and (37) using the Lin–Bairstow method [5], which gives the complex roots of polynomials. Figures 3 and 4 show the stability of the four- and five-point methods, respectively, for a wide range of τ_1 and τ_2.

3.7. *Accuracy*

We now consider the accuracy of the circuit solutions. Both schemes share the same representation of the first derivative, Eq. (17). Taylor expanding and eliminating terms, we obtain the truncation error for the first derivative of a second-order backward Euler scheme:

$$\frac{dQ}{dt} \approx Q' - \frac{\Delta t^2}{3} Q^{(iii)}. \tag{38}$$

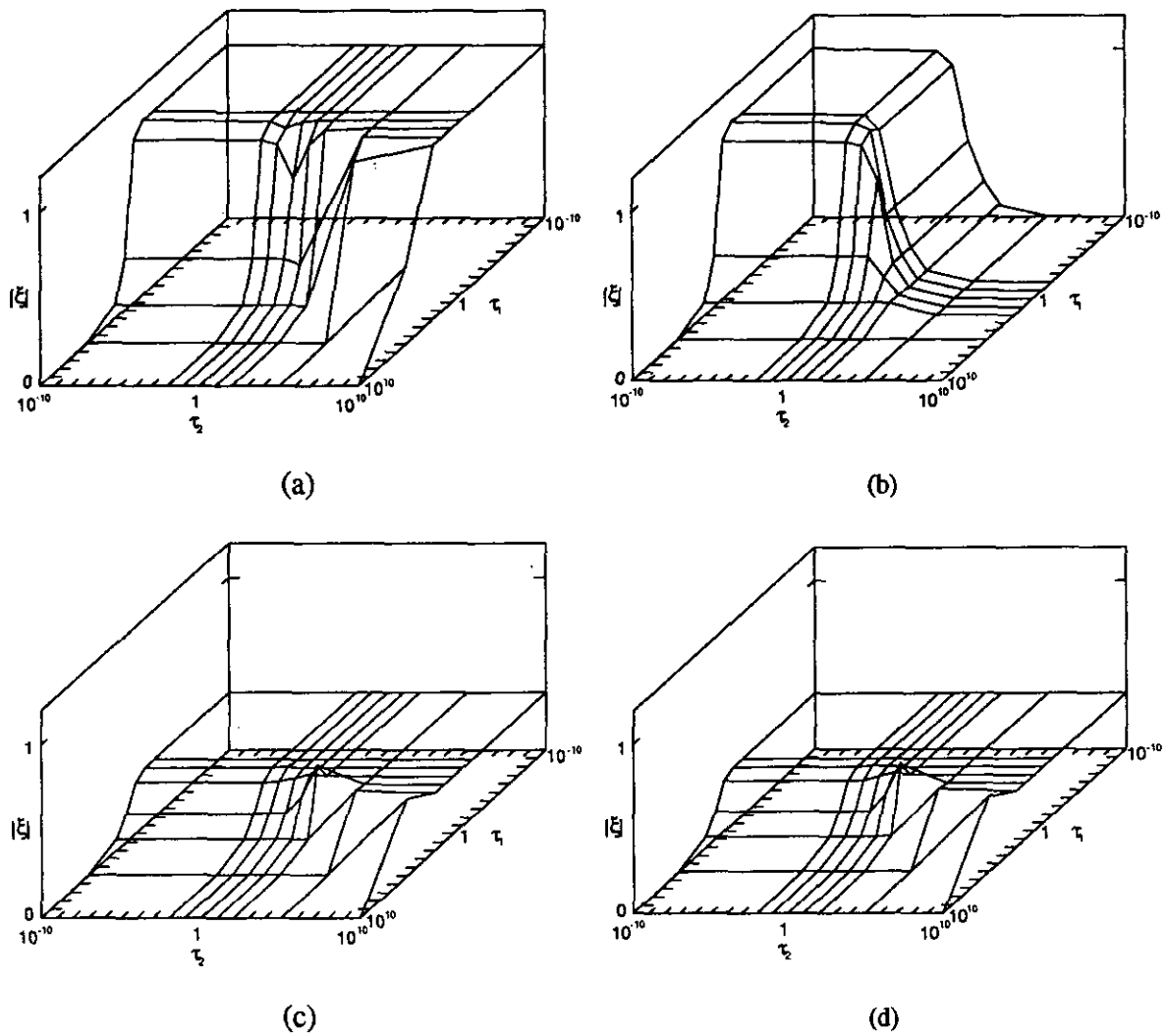

FIG. 4. Magnitude of the four stability roots of the five point method, whose characteristic equation is Eq. (37). Since all four roots, $|\xi_{1,2,3,4}| \leqslant 1$, the five-point difference scheme is stable over the range shown.

The truncation error for the second derivative using the five point scheme is given by

$$\frac{d^2Q}{dt^2} \approx Q'' - \frac{2\Delta t^2}{3} Q^{(iv)}. \tag{39}$$

Similarly, the truncation error for the second derivative using the four-point scheme is given by

$$\frac{d^2Q}{dt^2} \approx Q'' - \frac{11\Delta t^2}{12} Q^{(iv)}. \tag{40}$$

In comparison, the second-order scheme in [1] has a truncation error for the first derivative of $\Delta t^2 Q^{(iii)}/6$ and $\Delta t^2 Q^{(iv)}/12$ for the second derivative. The latter schemes are slightly more accurate when the stability criteria described in Section 1 are met. Note that when the inductive component is small, [1] switches to a first-order scheme with truncation error given by $-\Delta t Q''/2$ and decouples the circuit solution from the Poisson solution. Lawson [1] also proposes a method which corrects for the decay rate of a capacitor. This method results in a truncation error of $-\Delta t^2 Q''/2$ at the expense of decoupling the circuit solution from the Poisson solution and requiring a relaxation step to apply the boundary conditions.

4. CONCLUSION

A method for the simultaneous solution of the coupled potential and external circuit equations for one-dimensional electrostatic plasma particle simulations is presented. The method is stable over many orders of magnitude for the values of the RLC circuit elements and can, in principle, be extended to arbitrary external circuits.

The method improves on the accuracy and stability of the scheme of [1] for a large class of problems of current interest. However, this general improvement comes at the expense of a slightly reduced accuracy for the case of a circuit with non-neglible inductance. This is deemed an acceptable trade-off, especially for simulators interested in rf discharges and materials processing applications.

The method is implemented in the codes PDP1 (plasma device planar 1 dimension), PDC1 (cylindrical), and PDS1 (spherical) [6]. These codes have been used to simulate many complete bounded plasma devices [7–12], including voltage-driven rf discharges, plasma immersion ion implantation devices, and Q-machines. The codes have performed reliably, generating many interesting discussions and discoveries.

ACKNOWLEDGMENTS

We are grateful to W. S. Lawson for allowing us to borrow liberally from his code PDW1, as well as for providing numerous suggestions and discussions. We also thank E. Horowitz for his insight regarding particle weighting in curvilinear geometry. This work was supported in part by DOE Contract DE-FG03-86ER53220 and ONR Contract N00014-85-K-0809. This work was performed under appointment to the Magnetic Fusion Energy Technology Fellowship program which is administered for the U.S. Department of Energy by Oak Ridge Associated Universities.

REFERENCES

1. W. S. Lawson, *J. Comput. Phys.* **80**, 253 (1989).
2. C. K. Birdsall and A. B. Langdon, *Plasma Physics via Computer Simulation* (McGraw-Hill, New York, 1985).
3. W. H. Press, B. P. Flannery, S. A. Teukolsky, and W. Y. Vetterling, *Numerical Recipes in C* (Cambridge Univ. Press, Cambridge, UK, 1988).
4. C. W. Gear, *Numerical Initial Value Problems in Ordinary Differential Equations* (Prentice-Hall, Englewood Cliffs, NJ, 1971).
5. M. L. James, G. M. Smith, and J. C. Wolford, *Applied Numerical Methods for Digital Computation* (Harper and Row, New York, 1985).
6. Codes available through Software Distribution Office, Industrial Liason Program, Cory Hall, University of California, Berkeley, CA 94720.
7. M. V. Alves, V. Vahedi, and C. K. Birdsall, *Bull. Am. Phys. Soc.* **34**, 2028 (1989).
8. I. J. Morey, V. Vahedi, and J. P. Verboncoeur, *Bull. Am. Phys. Sec.* **34**, 2028 (1989).
9. I. J. Morey, V. Vahedi, and J. P. Verboncoeur, *Proceedings 13th Conference on the Numerical Simulation of Plasmas, 1989*, PMB 11 (1989).
10. M. V. Alves, V. Vahedi, and C. B. Birdsall, *Proceedings, 13th Conference on the Numerical Simulation of Plasmas*, PW11 (1989).
11. M. V. Alves, V. Vahedi, and C. K. Birdsall, *Proceedings, 42th Annual Gaseous Electronics Conference, 1989*, p.61
12. I. J. Morey, V. Vahedi, J. P. Verboncoeur, and M. A. Lieberman, *Proceedings, 42nd Annual Gaseous Electronics Conference, 1989*, p. 61.